Astronomy & Astrophysics manuscript no. sofia˙pillars˙30032012
September 25, 2018

Letter to the Editor

Globules and pillars seen in the [CII] 158 μm line with SOFIA

N. Schneider[1], R. Güsten[2], P. Tremblin[1], M. Hennemann[1], V. Minier[1], T. Hill[1], F. Comerón[3], M.A. Requena-Torres[2], K.E. Kraemer[4], R. Simon[5], M. Röllig[5], J. Stutzki[5], A.A. Djupvik[6], H. Zinnecker[7,8,9], A. Marston[10], T. Csengeri[2], D. Cormier[1], V. Lebouteiller[1], E. Audit[1], F. Motte[1], S. Bontemps[11,12], G. Sandell[7], L. Allen[13], T. Megeath[14], and R.A. Gutermuth[15]

(Affiliations can be found after the references)

September 25, 2018

ABSTRACT

Molecular globules and pillars are spectacular features, found only in the interface region between a molecular cloud and an H II-region. Impacting far-ultraviolet (FUV) radiation creates photon-dominated regions (PDRs) on their surfaces that can be traced by typical cooling lines. With the GREAT receiver onboard SOFIA we mapped and spectrally resolved the [C II] 158 μm atomic fine-structure line and the highly excited ^{12}CO J=11→10 molecular line from three objects in Cygnus X (a pillar, a globule, and a strong IRAS source). We focus here on the globule and compare our data with existing *Spitzer* data and recent *Herschel* open-time PACS data. Extended [C II] emission and more compact CO-emission was found in the globule. We ascribe this emission mainly to an *internal* PDR, created by a possibly embedded star-cluster with at least one early B-star. However, external PDR emission caused by the excitation by the Cyg OB2 association cannot be fully excluded. The velocity-resolved [C II] emission traces the emission of PDR surfaces, possible rotation of the globule, and high-velocity outflowing gas. The globule shows a velocity shift of ~2 km s^{-1} with respect to the expanding H II-region, which can be understood as the residual turbulence of the molecular cloud from which the globule arose. This scenario is compatible with recent numerical simulations that emphasize the effect of turbulence. It is remarkable that an isolated globule shows these strong dynamical features traced by the [C II]-line, but it demands more observational studies to verify if there is indeed an embedded cluster of B-stars.

Key words. interstellar medium: clouds – individual objects: Cygnus – molecules – kinematics and dynamics – Radio lines: ISM

1. Introduction

Molecular *pillars* and *globules* are visually spectacular features that are produced when the ionizing radiation from OB-stars forms elongated structures in the neutral gas at the interface between H II-regions and molecular clouds. Though known for a long time, these features were popularized by the *Hubble* Space Telescope (e.g. the famous 'Pillars of Creation' in M16). More recent *Herschel* observations from the HOBYS key program (Motte et al. 2010) have revealed many nice examples of *pillars* and *globules* in Cygnus-X, our SOFIA (Stratospheric Observatory For Infrared Astronomy) target. An important question is under which conditions which type of stars can form inside *pillars* and *globules*. So far, low-mass stars have been found (Sugitani et al. 2002) but to date no clear observational signature of more massive stars exists. In this *letter* we show observations that point toward the existence of a cluster of B-stars associated with a *globule*.

Pillars have a column-like shape and a physical connection to the gas reservoir of the molecular cloud while *globules* are isolated and have a head-tail structure pointing toward the illuminating source (see Fig. 1). Both are only found in regions of OB-stars where a direct impact of UV-radiation creates photon-dominated regions (PDRs) on the surface of a molecular cloud/clump, often visible as a bright rim at the edge of the cloud. These PDRs are best traced in their cooling lines, i.e. atomic fine-structure lines of ionized carbon ([C II] at 158 μm) and atomic oxygen ([O I] at 63 and 145 μm), as well as high-J CO rotational lines.

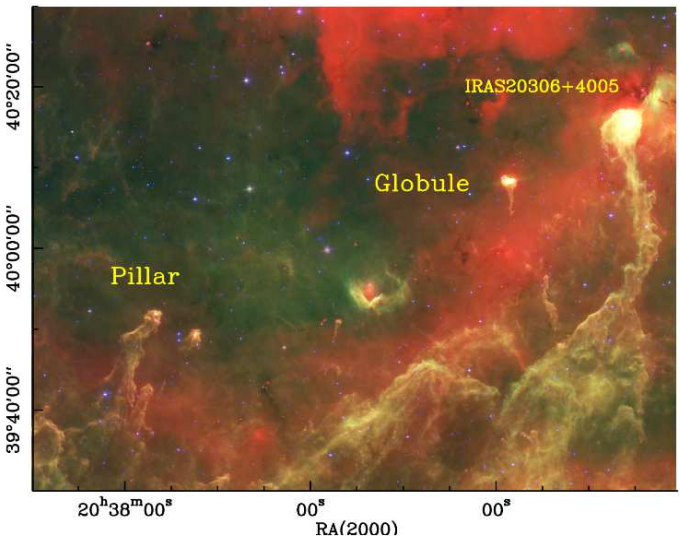

Fig. 1. Three-color (3.6, 8, and 24 μm) *Spitzer* image of the southern Cygnus-X region, obtained from the Cygnus-X legacy survey (Hora et al. 2009, http://www.cfa.harvard.edu/cygnusX). The Cyg OB2 association is located at a projected distance of ~1.2° north (≈40 pc, assuming a distance of 1.4–1.6 kpc, Rygl et al. 2012). The sources observed with SOFIA (pillar, globule, IRAS20306+4005) are as indicated.

The basic explanation for the formation of *globules* (e.g. Lefloch & Lazareff 1994) involves UV-radiation impacting on

a pre-existing clumpy molecular cloud and photoevaporating the lower density gas, leaving only the densest cores, which may collapse to form stars ('radiative driven implosion' scenario, Bertoldi 1989). Recent (magneto)-hydrodynamic simulations including radiation (Gritschneder et al. 2009, Tremblin et al. 2012a, 2012b) begin to successfully model *pillar/globule* formation from a different perspective, emphasizing the importance of turbulence.

To understand *pillar* and *globule* formation, in particular under which conditions stars can form within them, we initiated a large observational and numerical study. This program collects observations from a *Herschel* open time project[1], ground-based molecular line Mopra observations[2], and the SOFIA observations presented here. We use the HERACLES code (Gonzales et al. 2007) and the radiative transfer PDR-code KOSMA-tau (Röllig et al. 2006) for modeling.

The initial objective of the [C II] 158 μm and CO J=11→10 SOFIA observations was to obtain spectrally resolved data to study the effect of external UV-radiation on *pillars* and *globules*, and to interpret these in light of numerical simulations. We chose to focus on the southern part of the Cygnus-X region (Reipurth & Schneider 2008) where the very massive and rich Cyg OB2 association (with an estimated 2600 OB-stars, Knödlseder 2000) illuminates the molecular cloud (see Fig. 1).

2. Observations

The [C II] atomic fine-structure line at 1.90 THz (158 μm) and the CO J=11→10 molecular rotation line at 1.267 THz were observed with the PI-heterodyne receiver GREAT[3] on SOFIA on a flight 2011, November 10 from Palmdale, California. On-the-fly maps with a scanning speed of 6″/s and a size of 4′×3′ and 3.5′×1′ were made of the globule and the pillar, and the IRAS source, respectively. The globule was taken in two coverages, while the pillar and the IRAS source were observed in only one coverage. The pillar does not have a sufficient signal-to-noise (S/N) ratio, and the IRAS source is not fully covered, therefore we did not attempt a more quantitative analysis of these sources. We only use a spectrum of each (Fig. 6) here, because they assist our argument for globule formation. For blank sky-subtraction, an OFF-positions was used, based on molecular line and IR-surveys. A main-beam efficiency of 0.51 (L2 channel with [C II]) and 0.54 (L1 channel with CO) was applied to the data (Heyminck et al. 2012) and a linear baseline was removed. The observed rms level is 3.3 K (on a main beam temperature scale in a channel of 0.23 km s^{-1}), corresponding to a S/N ratio of ≈ 6 for the peak position. The absolute calibration uncertainty is estimated to be around 20 % (Heyminck et al. 2012).

In addition, [C II] 158 μm, [O I] 145 μm and 63 μm data from the aforementioned *Herschel* open time project were obtained for the globule on 2010, December 14, using the PACS spectrometer (Poglitsch et al. 2010). These observations consist of a single pointing (field of view 47″×47″) in chopping/nodding range scan mode, with a chopper throw of 6′ and Nyquist spectral sampling. The data were reduced using the standard reduction pipeline in HIPE 7.0. The final maps, from which the line fluxes are measured, were made with the PACSman software (Lebouteiller et al. 2012). These PACS maps (11.5″ at 158 μm) were then convolved to the approximate beamsize of SOFIA at 158 μm (16″) and the intensity ratio of individual positions was determined. The SOFIA [C II] data are typically a factor 1.6 stronger than the PACS data. Note, however, that PACS calibration was only derived from on-source data (the off-source position was contaminated by emission), and the calibration for SOFIA is still being tested. Despite this, the peaks of emission coincide very well, within 5″ (the PACS pointing accuracy is

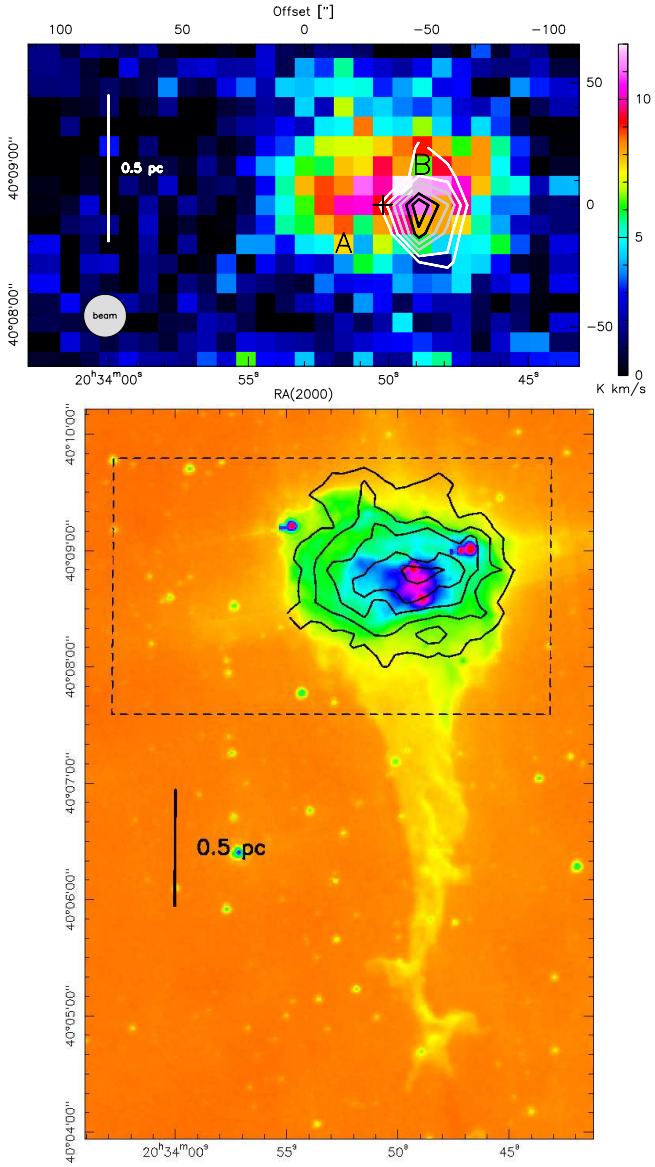

Fig. 2. Top: Map of [C II] emission (color-coded, integrated between 3 and 12 km s^{-1} in K kms^{-1} on a T_{mb} scale). The 0,0-position is RA(2000)=20^{h}33^{m}53^s Dec(2000)=40°8′45″. The contours (1 to 3.5 K kms^{-1} by 0.5 K kms^{-1}) indicate the very confined CO J=11→10 emission. **Bottom:** Overlay of [C II] contours (3 to 11 K kms^{-1} by 2 K kms^{-1} in a T_{mb} scale) in black on the *Spitzer* 5.8 μm continuum emission. The central cluster and a smaller sub-cluster in the northwest in the head of the globule (in pink) are clearly visible. The dashed rectangle indicates the area mapped in [C II]. Labels A, B, and the cross indicate the positions of the [C II] spectra shown in Fig. 4.

[1] 'Pillars of creation: physical origin and connection to star formation', PI: N. Schneider (PACS, SPIRE, and HIFI spectroscopy)

[2] Mopra PIs: P. Tremblin, V. Minier (CO, HCN, HCO$^+$ lines)

[3] The German REceiver for Astronomy at Terahertz frequencies. GREAT is a development by the MPI für Radioastronomie and the KOSMA/Universität zu Köln, in cooperation with the MPI für Sonnensystemforschung and the DLR Institut für Planetenforschung.

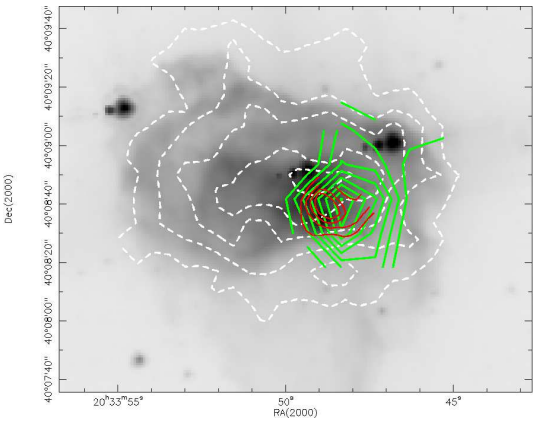

Fig. 3. Overlay of PDR-tracer lines on the *Spitzer* 5.8 μm continuum emission. White dashed contours: [C II] 158 μm levels 3 to 11 K kms^{-1} by 2 K kms^{-1}. Green contours: CO J=11→10 levels 1 to 3.5 K kms^{-1} by 0.5 K kms^{-1}. Red contours: [O I] 145 μm 0.7e-16 to 1.5e-16 by 0.2e-16 W/m^2.

≈2″), indicating that the pointing of SOFIA, using planets and optical pointing with a guide-camera, has been very reliable. Table 1 summarizes the flux values of each target from both sets of observations.

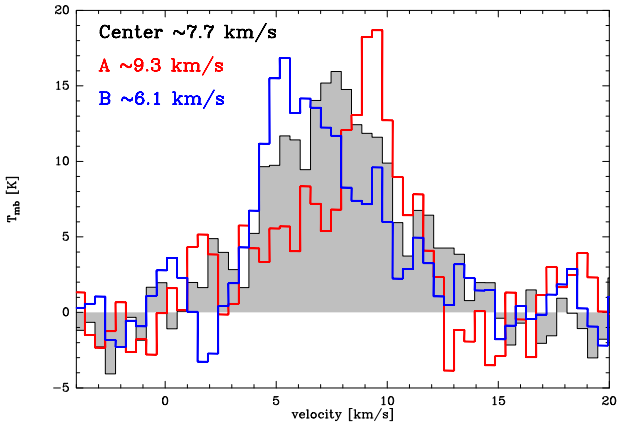

Fig. 4. Individual [C II] spectra from the globule (angular resolution 16″), with positions A, B, and center (+) as indicated in Fig. 2 (top). The velocities quoted in the panel are the line-center velocities obtained by a Gaussian fit. The 'center' spectrum has the broadest linewidth (6.7 km s^{-1}) compared to 4.0 and 4.9 km s^{-1} for positions 'A' and 'B'.

3. Results and analysis

The [C II] map of the globule and an overlay on *Spitzer* 5.8 μm emission is given in Figs. 2 and 3, whilst the [C II] spectra at three selected locations are found in Fig. 4. The [C II] emission covers the head of the globule with an increase in intensity toward the center. The CO J=11→10 emission is very confined in the southwest as is also seen in Fig. 3, showing a zoom of the globule head and where we additionally plot contour levels of *Herschel* PACS [O I] 145 μm emission. All PDR lines tracing in particular *warm* gas are confined in the same position. We overlay [C II] and *Spitzer* on a near-IR 2MASS image in Fig. 7 where both images reveal a number of compact sources that are located at the peak of [C II] and CO emission. This is a cluster with at least one early-type B-star (see appendix A for details). To what extent this cluster is embedded has a strong implication on the interpretation of the [C II] emission distribution.

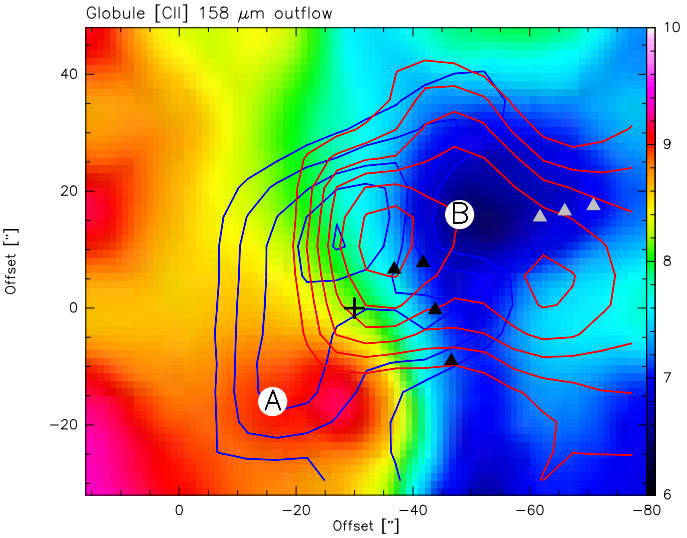

Fig. 5. Close-up of the [C II] map of the globule with the peak line velocity in color, determined from a Gaussian fit to each spectrum. From each Gaussian fit, the excess emission in the blue (~4 to 7 km s^{-1}) and redshifted (~9.5 to 11 km s^{-1}) wing was determined and is plotted as blue and red contours (for better visibility the maps are resampled on a finer grid). The black triangles indicate the cluster memebers within the H II-region (note that this is where the hot gas, visible in CO J=11→10 emission is found). The gray triangles mark the three sources from the secondary cluster.

Though it is clear, considering the orientation and shape of the globule, that the impact of the Cyg OB2 association (≈40 pc projected distance) created the globule, it is less obvious that the observed [C II] emission is only caused by *externally* illuminated PDRs. In this case, a limb-brightened, arc-like emission distribution with a decrease of intensity toward the center should be seen. In contrast, [C II] [O I] and CO peak where the brightest sources are found, arguing for *internal heating* due to the cluster. However, because we do see 2MASS sources with IR excess projected just outside the globule, it is possible that the globule was larger in the past, formed an extended cluster, and B-stars from this cluster are now outside the shrinking globule, illuminating it externally. This may explain why the [C II] emission is quite extended and not as confined as the CO and [O I] emission. On the other hand, beam dilution and exitation by UV-photons leaking out to the surface with clumps having a small area-filling factor might also serve as an explanation.

Studying the dynamics of the gas with the [C II] spectra (Fig. 4), however, supports the idea that at least most of the B-cluster is embedded. The 'center', located at the position of the cluster, represents the bulk emission of the globule around 7.7 km s^{-1} with a broad linewidth, suggesting that material is moving toward and away from us along the line-of-sight (LOS). The spectra of positions A and B show a symmetric – but opposite – velocity shift of 1.6–2 km s^{-1} along the LOS. Both spectra show high-velocity wing emission, i.e. a prominent red wing for

the blueshifted 'B' spectrum and the reverse situation for the 'A' position.

The velocity field of the central region of the globule is shown in Fig. 5. There is a sharp border between the two velocity ranges (~6 and 9 km s^{-1}), and the star-cluster is spatially located between these two velocity components. The velocity field shows a possible pattern of rotation around a slightly inclined northsouth axis of the globule, similar to what was already seen in CO-observations in *pillars* (Gahm et al. 2006, Hily-Blant et al. 2005). In addition, the globule is somewhat flattened orthogonal to the rotation axis, which could be interpreted as an additional argument for rotation. The minimum mass of the globule needed to support rotation is estimated from $M = (v^2 r)/G$) to 93 $M_\odot$ with a velocity v of 2 km/s and radius r 0.1 pc, which agrees with mass estimates from dust observations (see appendix A). Overlaid on the velocity field are blue and red contours of line-integrated [C II] emission from the two high-velocity wings, resulting in a typical 'outflow' pattern with two lobes. We attribute the high-velocity emission to warm gas that is accelerated by the expanding H II-region into an inhomogeneous environment. This scenario is similar to the one found in SOFIA [C II] observations of S106 (Simon et al. 2012).

The most probable explanation of the extended [C II] emission and the confined CO and [O I] emission is therefore a combination of internal heating by the cluster, clumpiness in the globule, and some contribution from the FUV flux from Cyg OB2. To quantify this scenario, we determined an FUV intensity of χ ≈390 at the position of the globule head using the IRAS 60 and 100 μm fluxes (Nakagawa et al. 1998). *External illumination* from Cyg OB2 can contribute to the flux, we estimated a range between χ ≈180–370, depending on the number of O-stars (see appendix B for details) but is unlikely. In contrast, *internal illumination* by at least one B-star produces a flux of χ ≈360 to 11000 (depending on the spectral type, see appendix A) in a distance of 0.1 pc from the star, which would be consistent with our observations.

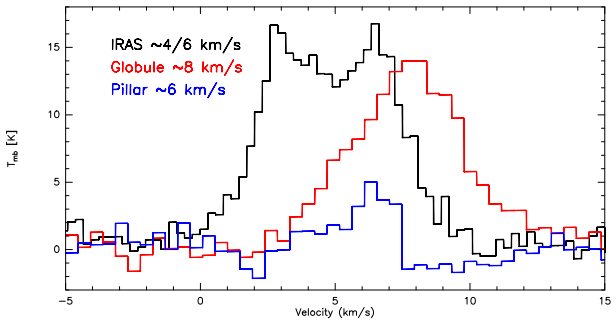

Fig. 6. Representative [C II] spectra from the three observed regions, the pillar, globule (center position with bulk emission) and IRAS20306+4005. The double-peaked spectrum from the IRAS source is due to two seperate components at around 4 and 6 km s^{-1}. The [C II] spectrum of the globule (red) shows a shift of around 2 km s^{-1} with respect to the pillar (blue) and IRAS source (black).

4. Formation of the globule

Comparing the [C II] spectra from the globule, pillar, and IRAS source (Fig. 6) shows that the globule has a velocity difference of ~2 km s^{-1} with respect to the other two sources. The pillar and the IRAS source are still attached to the molecular cloud (see Fig. 1) but directly face the expanding H II -region. We therefore define their velocity of ≈6 km s^{-1} as that of the expanding H II -region[4]. The velocity difference seen for the globule can then be understood from simulations (Tremblin et al., 2012b) as the residual turbulence of the molecular cloud. When the ionized gas pressure dominates the ram pressure of the initial turbulence in the molecular cloud, the dynamic is imposed by the expansion of the H II -region, leading to a global expansion, with the formation of clumps and pillars in the dense border-shell of the primordial molecular cloud. When the ram pressure of the turbulence exceeds the ionized gas pressure, the cold gas has sufficient kinetic energy to enter the H II -region with motions that are perpendicular to the ionization propagation. Then more globules are formed that show a typical velocity shift with respect to the cloud of a few km s^{-1}. The shift can be regarded as the remnant signature of turbulence inside the molecular cloud. This picture is quite different from a radiative-driven implosion scenario of isolated clumps, which does not predict any particular velocity difference.

	Flux [10 $^{-16}$ W m^{-2}]	Flux [10^{-5} erg s^{-1} cm^{-2} sr^{-1}]
SOFIA [C II] 158 μm	4.34	7.54
SOFIA ^{12}CO 11→10	0.7 (1.6)	1.21 (2.78)
PACS [C II] 158 μm	2.71	4.71
PACS [O I] 145 μm	1.24 (1.34)	2.15 (2.32)
PACS [O I] 63 μm	2.34 (2.51)	4.07 (4.36)

Table 1. Flux values from SOFIA and *Herschel* PACS observations of the globule. For comparison purposes, all maps have the same angular resolution of 16″. The fluxes were determined for the position –40″,0 (peak of [C II]) though for some lines, the value of the peak position is offset from this position (see Fig. 3and is given in parenthesis.

Acknowledgements. Based on observations made with the NASA/DLR Stratospheric Observatory for Infrared Astronomy. SOFIA Science Mission Operations are conducted jointly by the Universities Space Research Association, Inc., under NASA contract NAS2-97001, and the Deutsches SOFIA Institut under DLR contract 50 OK 0901.

References

Bertoldi, F., 1989, ApJ, 346, 735
Cohen, M., Jones, B.F., Walker, H.J., 1989, ApJ 341, 908
Comerón, F., Torra, J., 2001, A&A, 375, 539
Gahm, G.F., Carlqvist, P., Johansson, L.E., et al., 2006, A&A, 454, 201
Gonzales, M., Audit, E., Huynh, P., 2007, A&A 464, 429
Gritschneder, M., Naab, T., Walch, S. et al., 2009, ApJ, 694, L26
Hanson, M. M. 2003, ApJ, 597, 957
Heyminck, S., Graf, U.U., Güsten, R., Stutzki, J., et al., 2012, this issue
Hily-Blant, P., Teyssier, D., Philipp, S., Güsten, R., 2005, A&A, 440, 909
Holberg, J.B., Forrester, W.T., Shemansky, D., et al., 1982, ApJ 257, 656
Hora, J., Bontemps,S., Megeath, T., et al., 2009, Bull. of the AAS, 41, 356.01
Knödlseder, J., 2000, A&A, 360, 539
Kronberger, M., Teutsch, P., Alessi, B., et al., 2006, A&A, 447, 921
Kumar, M., Keto, E., Clerkin, E., 2006, A&A, 449, 1033
Lebouteiller, V., Cormier, D., Madden, S.C., 2012, A&A, submitted
Lefloch B., Lazareff B., 1994, A&A, 289, 559
Martin-Hernandez, N.L., Vermeij, R., van der Hulst, J.M., 2005, A&A, 433, 205
Motte, F., Zavagno A., Bontemps S., Schneider N., et al., 2010, A&A, 518, L77
Nakagawa, T., Yui, Y., Doi, Y. et al., 1998, ApJS, 115, 259
Odenwald, S. F., Campbell, M. F., Shivanandan, K., et al., 1990, ApJ, 99, 288

[4] This is confirmed by CO 3→2 data that will be shown in a forthcoming paper.

Panagia, N., 1973, AJ, 78, 929
Poglitsch, A., Waelkens, C., Geis, N., et al., 2010, A&A 518, L2
Reipurth, B., Schneider, N., 2008, Handbook of star-forming regions, ASP, p.37
Röllig M., Ossenkopf V., Jeykumar S., et al., 2006, A&A 451, 917
Roy, A., Ade P., Bock, R., et al., 2011, ApJ, 727, 114
Rygl, K., Brunthaler, A., Sanna, A., et al. 2012, A&A 539, 79
Setia Gunawan,A.,de Bruyn,A.,van der Hucht,K., et al.,2003,ApJS,149,123
Simon, R., Schneider, N., Stutzki, J., et al., 2012, this issue
Sridharan, T.K., Beuther, H., Schilke, P., et al., 2002, ApJ, 566, 931
Sugitani K., Tamura, M., Nakajima, Y., et al., 2002, ApJ 565, L28
Tremblin, P., Audit, E., Minier, V., Schneider, N., 2012, A&A, 538, 31
Tremblin, P., Audit, E., Minier, V., Schmid, W., Schneider, N., 2012, A&A sub.
van Leeuwen, F., 2007, A&A, 474, 653
Williams, S., Fuller, G., Sridharan, T.K., 2005, A&A, 434, 257

---

[1] IRFU/SAp CEA/DSM, Laboratoire AIM CNRS - Université Paris Diderot, 91191 Gif-sur-Yvette, France
[2] Max-Planck Institut für Radioastronomie, Bonn, Germany
[3] ESO, Karl Schwarzschild Str. 2, 85748, Garching, Germany
[4] Boston College, Institute for Scientific Research, MA 02467, USA
[5] KOSMA, I. Physik. Institut, Universität Köln, Köln, Germany
[6] NOT, 38700 Santa Cruz de la Palma, Spain
[7] SOFIA-USRA, NASA Ames Research Center, Moffett Field, CA 94035, USA
[8] Astrophysikalisches Institut Potsdam, 14482 Potsdam, Germany
[9] Deutsches SOFIA Institut, Universität Stuttgart, Germany
[10] Herschel Science Centre, ESAC, ESA, Madrid, Spain
[11] Univ. Bordeaux, LAB, UMR 5804, F-33270 Floirac, France
[12] CNRS, LAB, UMR 5804, F-33270 Floirac, France
[13] National Optical Astronomy Observatory, Tucson, AZ 85719, USA
[14] Dep. of Physics and Astronomy, U. of Toledo, OH 43606, USA
[15] Dep. of Astronomy, U. of Massachusetts, Amherst MA USA

Appendix A: The IR cluster

Figure 7 shows a near-IR image from 2MASS[5] with contours of *Spitzer* and [C II] overlaid. There is a higher stellar density at the location of the [C II] emission, coinciding well in size, shape, and position. There is substantial crowding in the 2MASS images and most of the fainter stars are typically red. On the red optical plates from the Digital Sky Survey only a handful of stars are seen. The extended emission seems brighter in the K-band. Judging from a preliminary J–H vs. H–K diagram, limited by source-confusion and sensitivity, the central cluster has a higher fraction of near-IR excess sources compared to the surrounding field. A preliminary color-color diagram also shows that sources with very different extinction values in the central cluster are found, though the median value is about 10 mag of visual extinction of the 2MASS sources measured. Many of the faint sources detected by 2MASS have no reliable flux measurement, however, and to make a detailed study of this cluster we need higher spatial resolution and deeper JHK images.

Based on these 2MASS images, both Kronberger et al. (2006) and Kumar et al. (2006) classified the crowding of stars as 'an associated, partly embedded cluster'. The latter give 9 cluster members within an effective radius of 0.53 pc, and a stellar mass of 17 $M_\odot$. Optical spectroscopy (Cohen et al. 1989) identified a B3 III star as one cluster member, but the spectral type classification is very uncertain because it comes from a rough fit to Balmer line depths, and the luminosity class III is derived from the required flux and not from a proper spectral classification.

Sridharan et al. (2002) derived a flux of 25 mJy at 3.6 cm and 1.4 Jy at 1.1 mm for this star, which is resolved at both wavelengths, and they interpreted it as a 90 $M_\odot$ clump comprising a high-mass protostellar object and an H II-region. Independently, the spectral type of the ionizing source can be estimated from the relation between the radio continuum flux density and the Lyman photon flux (Martin-Hernandez et al. 2005). A flux of ~13.7 mJy at 1.4 GHz has been measured (Setia Gunawan et al. 2003), which is consistent – as is the flux information at 3.6 cm – with an ionizing photon flux of F=1.8×10^{45} ph s^{-1}, i.e. a B1 ZAMS star according to Panagia (1973).

Low-angular resolution millimeter continuum observations (BLAST, Roy et al. 2011; SCUBA, Williams et al. 2005) indicate a dust temperature of 38 K and a lower limit of the total mass of about 40 $M_\odot$. Williams et al. determined a B2 spectral type from a luminosity of 4000 $L_\odot$ and dust modeling. Using data from recent *Herschel* imaging within the HOBYS program (Motte et al. 2010), we obtained a total mass of 80 $M_\odot$ for the globule (size scale ≈0.5 pc).

Though the spectral classification of the internal B-star is fairly uncertain (see above), we can estimate a flux considering different spectral types. Far-ultraviolet fluxes for a number of early B-type stars, which include α Vir (B1IV), α Eri (B3V), and β Cen (B1III), were measured by Holberg et al. (1982) using the UV spectrometers onboard the Voyager interplanetary probes. The spectral types of those three stars bracket the one estimated for the star at the center of the cluster, and their FUV luminosities can thus be taken as upper or lower limits to the UV radiation internally injected in the globule. We used the distances to these stars as determined by Hipparcos (van Leeuwen 2007) to obtain their luminosities in the 912 Å - 1225 Å range. We obtained luminosities of 1.1×10^{48} ph/s (α Vir), 9.7×10^{46} ph/s (α Eri), and 3.0×10^{48} ph/s (β Cen). The corresponding volume-averaged values of χ, adopting a typical radius of 0.2 pc for the globule, are χ=4,000 (α Vir), χ=360 (α Eri), and χ=11,000 (β Cen). These values are higher, or at least comparable for the lower limit set by the B3V star α Eri, than the peak value of χ derived from the IRAS 60 and 100 micron fluxes, thus supporting an internal origin for the excitation of the PDR.

[5] The Two Micron All Sky Survey (2MASS) is a joint project of the University of Massachusetts and the Infrared Processing and Analysis Center/California Institute of Technology, funded by the National Aeronautics and Space Administration and the National Science Foundation.

Appendix B: Estimation of UV-flux from Cyg OB2

We here consider only O-stars because they dominate the UV emission over B-stars, with O6 stars dominating the overall emission output from the cluster. The number of O-stars in Cyg OB2 is very uncertain and estimates range between ~45 and ~100 (see Reipurth & Schneider 2008 for an overview). In our estimates, we assume that $G_0 = 10^6$ at a distance of 0.1 pc from an O-star. The projected distance from the center of the OB association to the globule is 40 pc. Hence, 100 O-stars produce a flux of $G_0 \simeq 10^8/400^2 = 625$ at the position of the globule, corresponding to $\chi \simeq 370$. We consider this a strict upper limit. For 50 O-stars, this reduces to $G_0 \simeq 313$ or $\chi \simeq 183$.

The flux from the IRAS 60 and 100 μm flux ratio is $G_0 = 660$ or $\chi \simeq 390$ (obtained with a method described in Nakagawa et al. 1998) in a large beam at the position of the globule, which agrees well with the values estimated above. We believe, however, that the contribution to the FUV flux from the Cyg OB2 association is significantly lower than the upper limit derived above due to the reasons detailed below.

Because the volume around the OB association is not empty, there is still extinction on the way to the globule, which then does not receive the full UV flux from the entire O-star population. Unfortunately, it is not possible to give a precise quantification of the effect of extinction, but a reduction of the estimate of the flux by a factor of a few is possible.

A basic problem in estimating the number of O stars is the assumption of a single age for the whole association. Knödlseder (2000) used 3 Myr and thus assumed that all stars are on the main sequence, with the brightest stars, therefore, being hottest. Hanson (2003) already showed that some of the stars are bright because they are (B-type) giants and supergiants, not because they are hot. There are currently around 70 spectroscopically confirmed O stars in the association, but more than half of them are O8-O9.

Although it is already difficult to specify a distance between the O-stars and the globule, the distance of 40 pc to the center of the association is a *projected* distance. Taking into account the depth along the line of sight can only increase the actual distance, and because the external flux decreases quadratically with the distance to the cluster, this in addition may significantly decrease the FUV flux received by the globule.

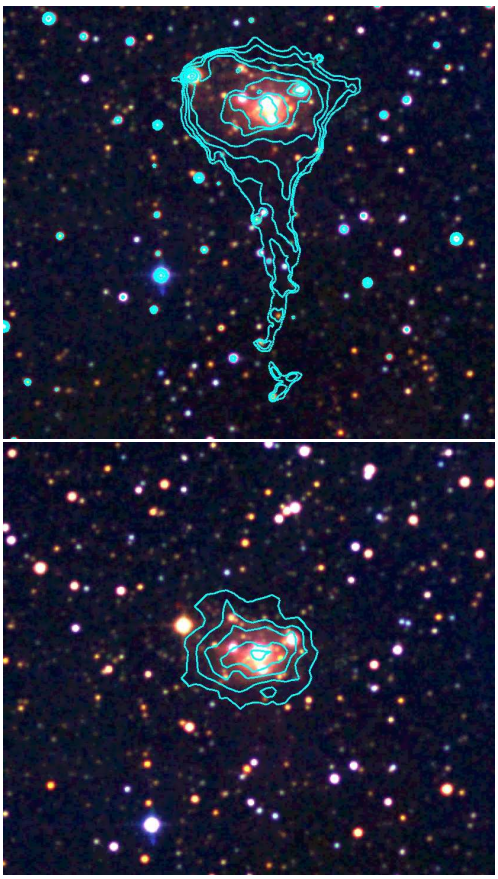

Fig. 7. Near-IR image of the 6′×6′ field centered on the cluster in the globule (RGB coded from 2MASS Ks, H and J) with contours (28, 30, 35, 50, 125, 200, and 600 MJy/sr) of the *Spitzer* 5.8 μm image (top) and the [C II] (bottom) contours (3-11 K km/s in steps of 2 K km/s) overlaid on it. North is up, east is left.